An efficient method for AVO modeling of reflected spherical waves

Chuck Ursenbach and Arnim B. Haase, CREWES, University of Calgary, and Jonathan E. Downton, Veritas DGC*

Summary

A method is presented for efficiently and accurately calculating the spherical-wave generalization of the Zoeppritz P-wave reflection coefficients. The main assumptions are that the wavelet is an exponential form that allows for analytic integration over frequency, and the direction of propagation and arrival time are as dictated by ray theory. These assumptions result in calculations sufficiently rapid to be carried out interactively on the computer. Results for an AVO Class I model show that this method quantitatively reproduces exact spherical-wave reflection coefficients obtained using a Ricker wavelet.

Introduction

This paper is concerned with reflected spherical waves in a two-layer elastic model, illustrated in the diagram below:

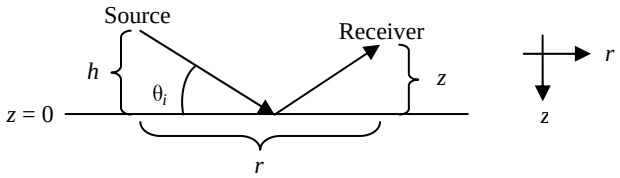

The plane-wave reflection coefficient for this system is the well-known Zoeppritz expression, $R_{PP}(p;\alpha_1,\beta_1,\rho_1;\alpha_2,\beta_2,\rho_2)$, where p is a ray parameter (the horizontal slowness), α, β, and ρ are P-wave velocity, S-wave velocity, and density, and subscripts 1 and 2 refer to upper and lower media. The generalized reflection coefficient associated with spherical waves, which includes contributions from both reflected and head waves, is obtained from an integral over $R_{PP}(p)$. The fundamental theory is well-established and is given, for example, by Aki and Richards (1980). They express the frequency-dependent potential as a weighted integral over all ray parameters of cylindrical waves times plane-wave reflection coefficients. In analogy with their Eq. (6.30) for free surface reflections, the pertinent expression for reflections from a solid-solid interface can be written as

$$\phi(\omega) = Ai\omega \exp(-i\omega t)\int_0^\infty R_{PP}\left(p;\alpha_1,\beta_1,\rho_1,\alpha_2,\beta_2,\rho_2\right)\frac{p}{\xi}J_0(\omega pr)\exp[-i\omega\xi(z+h)]dp. \quad (1)$$

Here A is a scaling factor, ω is the frequency, t is time, ξ is the vertical P-wave slowness in the upper layer, J_0 is the zero-order Bessel function, r is the horizontal receiver coordinate (with the horizontal source position equal to zero), h is the source elevation, and z is the vertical receiver coordinate.

The displacement is obtained by applying a gradient in the receiver position to the above potential. Weighting this by the wavelet and applying an inverse Fourier transform yields the displacement time trace observed at the receiver from which AVO information can be extracted. The above method has been implemented in numerical calculations by Haase (2004). Our objective in this study is to develop a semi-analytic approximation that is both highly efficient and quantitatively accurate.

Theory

Starting from Eq. (1) the time-domain potential can be written as $\Phi(t) = \int_{-\infty}^{\infty} f_n(\omega)\phi(\omega)d\omega$. In this expression $f_n(\omega)$ is the wavelet, defined to be of the form $f_n(\omega) \propto |\omega|^n \exp\left(-\frac{n|\omega|}{\omega_m}\right)$, where $n = 0, 1, 2, ...,$ and $\omega_m > 0$. For $n > 0$, $f_n(\omega)$ has a maximum at $\omega = \omega_m$.

The order of p and ω integrations is next interchanged[1], as shown here:

[1] Bortfeld (1962) justifies changing the order of integration for this integral. He develops a method in which a sinc function wavelet is employed for the integration over frequency, and the actual seismic wavelet is introduced at the end of the procedure by convolution. His method is therefore more general than the present approach, but also more computationally intensive.

Spherical-wave AVO

$$\begin{aligned}\Phi(t) &= \int_{-\infty}^{\infty} |\omega|^n \exp\left(-\frac{n|\omega|}{\omega_m}\right)\left[Ai\omega \exp(-i\omega t)\int_0^{\infty} R_{\mathrm{PP}}(p)\frac{p}{\xi} J_0(\omega p r)\exp[-i\omega\xi(z+h)]dp \right] d\omega \\ &= Ai\int_0^{\infty} R_{\mathrm{PP}}(p)\left[\int_{-\infty}^{\infty} \omega|\omega|^n J_0(\omega p r)\exp\left(-\frac{n|\omega|}{\omega_m} - i(t+\xi[z+h])\omega\right) d\omega \right]\frac{p}{\xi}dp \\ &\equiv Ai\int_0^{\infty} R_{\mathrm{PP}}(p)\left[I_R(p,\xi(p);\ n,\omega_m,r,z,h,t)\right]\frac{p}{\xi}dp.\end{aligned} \tag{2}$$

In the last step $I_R(p,t)$ is defined as the result of integration over ω (and for brevity the other variables are suppressed). It can be shown to be real. It is advantageous to change the lower bound of the ω-integration to zero. This leads directly to the analytic or complex trace, whose real part is proportional to the original integral. Effectively $I_R(p,t)$ in Eq. (2) is replaced with $I(p,t) = ½ [I_R(p,t) + i\, I_I(p,t)]$, where $I_R(p,t)$ and $I_I(p,t)$ are real functions. Changing the lower bound to zero also allows |ω| to be replaced by ω, and gives the integral the form of a Laplace transform for which an analytic solution is available (Erdelyi, 1954):

$$I(p,t) = \frac{(n+1)!}{\tau^{n+2}} P_{n+1}\left(\frac{T}{\tau}\right), \quad \text{where } T = \frac{n}{\omega_m} + i(t+\xi[z+h]), \quad \tau = \sqrt{T^2 + p^2 r^2}, \quad \text{and } P_n(x) \text{ is a Legendre function.} \tag{3}$$

Next one applies a gradient to obtain displacement of the reflected wavefield, $U(t) = \nabla\Phi(t)$. Assuming that displacement is in the direction of propagation of the reflected wave, one can begin by substituting $z = -R\cos(\theta_i) - h$ and $r = R\sin(\theta_i)$, which effectively defines θ_i as the angle of incidence and R as the distance traveled by the wave. Then the desired gradient is obtained by differentiating with respect to R. All geometry dependence is contained within $I(p,t)$, so this means simply replacing it with $\partial I(p,t)/\partial R$ in the integral. Note that the assumption regarding the direction of the reflected wave may not be valid near the critical point, where it co-exists with the head wave. However, the difference is expected to be small, and this assumption is tested below.

Eq. (2) is a function of time, t. Assuming that the signal of interest from the interface will arrive at the receiver at time R/α_1, let $t = R/\alpha_1$ so that only $U(R/\alpha_1)$ is calculated. (The discussion in the last paragraph regarding the critical point applies here as well, and this arrival time assumption is also tested below.)

In order to compare the spherical-wave reflection coefficients meaningfully with the plane-wave results, it is necessary to normalize out the divergence effects, etc. The simplest way to calculate a normalization factor is to recalculate $U(R/\alpha_1)$ with the plane-wave R_{PP} set to unity. This quantity, denoted $U(R/\alpha_1; R_{\mathrm{PP}}=1)$, has an analytic form. Dividing the unnormalized coefficient by this new quantity removes all effects except the actual reflection at the interface, and the result is denoted $R_{\mathrm{PP}}^{\mathrm{sph}}(\theta_i) \equiv U(R/\alpha_1) \div U(R/\alpha_1; R_{\mathrm{PP}}=1)$. In practice the quantity $\partial I(p,t)/\partial R$ can be divided by the normalization factor prior to integration over p, and the results are collected together into the expression

$$\begin{aligned}R_{\mathrm{PP}}^{\mathrm{sph}}(\theta_i) &= \int_0^{\infty} R_{\mathrm{PP}}(p;\alpha_1,\beta_1,\rho_1,\alpha_2,\beta_2,\rho_2)\left[\frac{1}{\alpha_1}\frac{Ai}{U(R/\alpha_1;R_{\mathrm{PP}}=1)}\frac{\partial I(p,t)}{\partial R}\bigg|_{t=R/\alpha_1}\right]\alpha_1\frac{(\sin\theta)/\alpha_1}{(\cos\theta)/\alpha_1}d\left(\frac{\sin\theta}{\alpha_1}\right) \\ &= \int_0^{\infty} R_{\mathrm{PP}}(\theta;\text{elastic parameters})W_n(\theta;\theta_i,R\omega_m/\alpha_1)\tan\theta\, d(\sin\theta).\end{aligned} \tag{4}$$

The complex function $W_n(\theta)$, as defined by Eq. (4), has a number of key properties. As shown in Figure 1, it peaks near the angle of incidence, and when multiplied by tanθ its real part is normalized to unity while its imaginary part integrates to zero. It thus acts as a weighting function to form a spherical-wave reflection coefficient from plane-wave coefficients in the vicinity of θ_i. It becomes narrower as the radius of curvature increases, approaching a delta function in the plane-wave limit. Finally, it has a programmable, closed-form expression for appropriate values of n, making it a useful quantity in modeling spherical-wave AVO.

Application

Consider a two-layer model with earth parameters specified in Table I. This constitutes a Class I AVO system, and it possesses a critical point at ~ 43.0°. Haase (2004) has employed an Ormsby wavelet to study the reflection coefficients of spherical waves in

this model. The Ricker wavelet is also in common use in exploration seismology (Sheriff, 2002). It can be written as $f_{\text{Ricker}}(\omega) = \omega^2 \exp\left[-(\omega/\omega_m)^2\right]$, and has a maximum at ω_m. Figure 2 shows that this can be approximated by the $f_n(\omega)$ wavelets.

Following Haase, this study employs a depth of $z = h = -500$m, and an overburden P-wave velocity of $\alpha_1 = 2000$ m/s (see Table I below). This, together with ω_m, specifies $R\omega_m/\alpha_1$, a combination of variables that occurs repeatedly in the final expressions for $W_n(\theta)$. It is equivalent to the quantity kr employed with monochromatic spherical waves, and determines the degree of deviation from plane wave behavior.

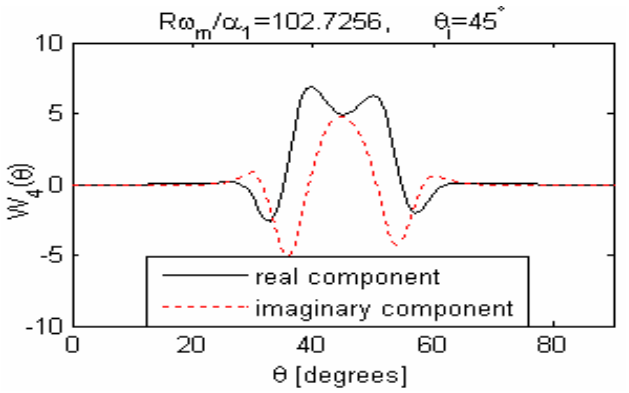

Figure 1: The normalized weighting function, $W_n(\theta)$, for particular values of R, ω_m, α_1, and θ_i.

Table I. Earth parameters for a two-layer, Class I AVO model. Other relevant parameters are $z = h = -500$ m, and $\omega_m/(2\pi) = 23.1$ Hz for the Ricker and exponential wavelets (see Figure 2). The Ormsby wavelet is defined by the parameters 5/15-80/100 Hz.

	Upper Layer	Lower Layer
α (m/s)	2000	2933.33
β (m/s)	879.88	1882.29
ρ (kg/m3)	2400	2000

The integrand of Eq. (4) includes two factors: (1) R_{PP}, which depends on elastic parameters of the two earth layers, and on the integration variable, and (2) W_n, which depends on the wavelet parameter n, on the combination $R\omega_m/\alpha_1$, on θ_i, and on the integration variable. Because the only dependence they share is the integration variable and α_1, it is possible to implement Eq. (4) efficiently. For plotting, the calculation of Eq. (4) is repeated for each incidence angle from 0° to 85° in 1° intervals.

Spherical-wave results in this paper have been calculated using two different methods, the semi-analytical weighting function method of Eq. (4), and, for purposes of comparison, the fully numerical approach of Haase (2004). Exponential wavelets have been employed with both methods, but the Ormsby and Ricker wavelets can only be handled by Haase's method.

Figure 3 shows spherical-wave results for two wavelets along with plane-wave results. There are significant amplitude deviations near the critical point, as noted by Haase (2004). The $f_5(\omega)$ wavelet appears to give a stronger spherical effect than the Ormsby wavelet. The Ormsby wavelet displays some oscillatory character just past the critical point. This is likely related to the slope discontinuities in the Ormsby wavelet. Both wavelets yield a qualitatively similar deviation from the plane wave result, so that spherical effects are only mildly dependent on the precise shape of wavelet.

Figure 4 shows a comparison of the results for the Ricker wavelet and three exponential wavelets. While all the plots agree well for most θ_i, there is essentially quantitative agreement is between the $f_5(\omega)$ and Ricker wavelets for this model.

Figure 5 displays the difference between the $f_5(\omega)$ and Ricker wavelets. The maximum difference in this case is < 0.01, which is negligible in practice. Two other small quantities are also plotted. One is the difference in $|R_{PP}|$ when the $f_5(\omega)$ wavelet is calculated by Haase's full numerical method and by Eq. (4). Essentially this constitutes a measure of the error introduced by setting $t = R/\alpha_1$ rather than calculating the entire trace and finding t_{max}. The other line is obtained by calculating the displacement perpendicular to the ray for the $f_4(\omega)$ wavelet (using a modification of Haase's method). It is essentially a measure of the error introduced by assuming that all displacement is parallel to the direction of propagation. In all cases the largest errors are found just after the critical point. It is in this region that the head-wave is beginning to separate from the reflected wave, but the two are still overlapping. Propagation directions and times are thus slightly different than ray theory predictions. The overall errors are small in absolute terms for this case, justifying the use of Eq. (4) for practical calculations.

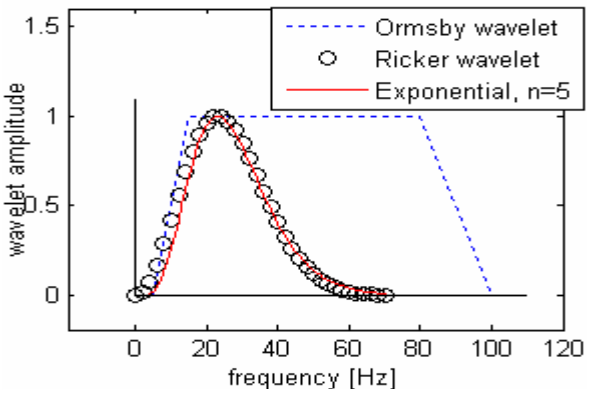

Figure 2: Three of the wavelets employed in this study. Ricker and exponential wavelets possess the same maximum. They in turn mimic the lower frequency amplitudes of the Ormsby wavelet.

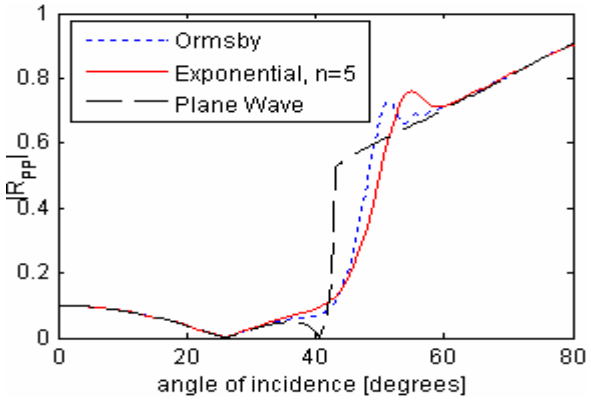

Figure 3: Reflection coefficient curves for Table I parameters. Spherical-wave coefficients are given for Ormsby and exponential wavelets, and are compared with plane-wave coefficients.

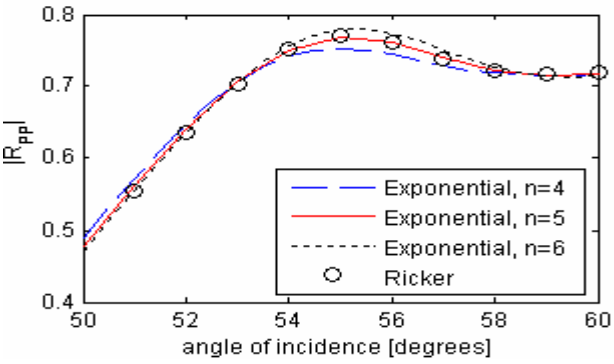

Figure 4: Comparison of Ricker and exponential wavelet effects.

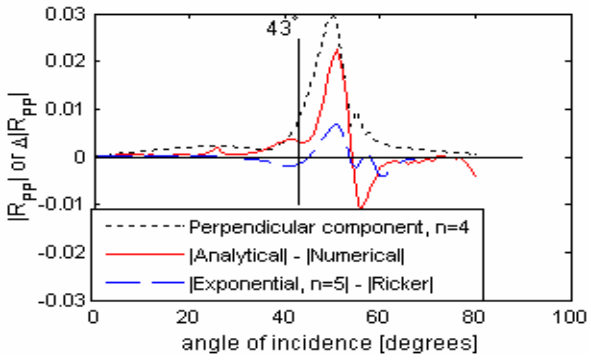

Figure 5: Representations of the principal errors in Eq. (4).

Conclusions

A new approximation has been presented in which spherical-wave reflection coefficients are shown to be a weighted integral of plane-wave coefficients near the angle of incidence. The method assumes an exponential form of the wavelet. This wavelet approximation can quantitatively mimic exact calculations using Ricker wavelets, and can qualitatively represent Ormsby wavelet results.

References

Aki, K. and Richards, P.G., 1980, Quantitative Seismology: Theory and Methods: W.H. Freeman, 1980.

Bortfeld, R., 1962, Reflection and Refraction of Spherical Compressional Waves at Arbitrary Plane Interfaces: Geophys. Prosp., **4**, 517-538.

Erdelyi, A., 1954, Tables of Integral Transforms, Vol. I, p. 182, New York, McGraw-Hill.

Haase, A.B., 2004, Spherical Wave AVO Modelling of Converted Waves in Elastic Isotropic Media, CSEG Expanded Abstracts.

Sheriff, R.E., 2002, Encyclopedic Dictionary of Applied Geophysics: SEG, 2002.

Acknowledgments

The authors express appreciation to Dr. E. Krebes for valuable discussions and suggestions in connection with this work.